
DEEPTRACK: LIGHTWEIGHT DEEP LEARNING FOR VEHICLE PATH PREDICTION IN HIGHWAYS

A PREPRINT

Mohammadreza Baharani
The UNC at Charlotte
Charlotte, NC
mbaharan@uncc.edu

Vinit Katariya, The UNC at Charlotte
Charlotte, NC
vkatariy@uncc.edu

Nichole Morris
University of Minnesota
Minneapolis, MN
nlmorris@umn.edu

Omidreza Shoghi
The UNC at Charlotte
Charlotte, NC
oshoghi@uncc.edu

Hamed Tabkhi
The UNC at Charlotte
Charlotte, NC
htabkhiv@uncc.edu

August 3, 2021

ABSTRACT

Vehicle trajectory prediction is an essential task for enabling many intelligent transportation systems. While there have been some promising advances in the field, there is a need for new agile algorithms with smaller model sizes and lower computational requirements. This article presents DeepTrack, a novel deep learning algorithm customized for real-time vehicle trajectory prediction in highways. In contrast to previous methods, the vehicle dynamics are encoded using Agile Temporal Convolutional Networks (ATCNs) to provide more robust time prediction with less computation. ATCN also uses depthwise convolution, which reduces the complexity of models compared to existing approaches in terms of model size and operations. Overall, our experimental results demonstrate that DeepTrack achieves comparable accuracy to state-of-the-art trajectory prediction models but with smaller model sizes and lower computational complexity, making it more suitable for real-world deployment.

1 Introduction

With the advent of high-speed communication systems and unprecedented improvements in trajectory predicting, we are closer to implementing a fully connected (vehicle-to-vehicle (V2V) and Vehicle-to-Infrastructure (V2I)) and fully-aware transportation system than ever before. The increasing push towards autonomous driving and thrust for designing the best in class crash-avoidance systems at the edge has resulted in developing trajectory forecasting algorithms with better than 90% accuracy for up to 5 seconds in the future. The use of such high accuracy models in safety-critical systems for crash avoidance and accident prediction can result in precise Time-to-Collision (TTC) prediction, which can prove instrumental in avoiding accident-related injuries and saving many lives.

In 2019, there were 36,096 fatalities on roadways in the United States [1, 2]. Of those fatal crashes, NHTSA (2019) estimates that 11.9% of them involved a vehicle maneuvering in a manner that may be unpredictable to the other drivers (i.e., turning left or right, stopping or slowing in traffic, merging/changing lanes, or passing another vehicle). Such crashes at highway speeds, given the short TTC and limited distance range, cannot be prevented with vision-based systems alone [3]. Providing enough time and distance to support effective crash avoidance via V2V systems must also utilize high-accuracy predictions for changing vehicle trajectories.

Predicting multiple possible trajectories for an active subject in the scene [4, 5] is a common practice. These trajectories are ranked based on the probability distribution of the prediction model, which may not be helpful in a real-time scenario. Hence, a deep learning algorithm for vehicle trajectory forecasting in a real-time safety-critical application must provide a single trajectory with high precision. It is imperative to consider the interactions of the surrounding

automobiles [6, 4] to successfully predict the accurate path of a moving vehicle in a highly dynamic environment. However, designing a real-time system at the edge for predicting safety-critical situations, the size and complexity of the model must also be considered. Smaller size and lower complexity result in faster predictions which can prove to be crucial in accident avoidance.

This article proposes DeepTrack as a novel deep learning model with comparable accuracy to best-in-class trajectory prediction algorithms but a much smaller model size with lower computational complexity to suit the resource-crunched embedded edge systems. DeepTrack encodes the vehicle dynamics with the aid of Agile Temporal Convolutional Networks (ATCN) instead of well-established LSTM units. ATCN, with its depthwise convolution as its backbone, can shrink the complexity of models and boost gradient flow for a more generalized trained model compared to LSTM-based solutions. Compared to CS-LSTM and its other variant CS-LSTM (M) [5], DeepTrack reduces prediction error by 9.09% and 11.56%, respectively, and reduces the number of operations and model size by about 10.49% and 18.5%, respectively. Concerning CF-LSTM [7], DeepTrack error raised for 0.87%; however, it can reduce the number of operations and model size by 10.49% and model size by 18.5%.

This article is organized as follows: Section 2 reviews the literature. Section 3 presents DeepTrack and introduces ATCN as an alternative to LSTMs used as dynamic encoders of vehicle trajectories to reduce model complexity. On both the accuracy and complexity of DeepTrack’s model, we compare the results to those of state-of-the-art solutions in Section 4. Finally, the chapter concludes in Section 5.

2 Related Work

Vehicle trajectory prediction networks are classified into three types, Physical-based, Maneuver-based, and Interaction-aware models [8]. The physical-based models are designed using the laws of physics, maneuver-based models consider the driver intentions, and interaction-aware models take surrounding vehicles and their interactions into account for motion and path prediction. Although interaction-aware models predict with a better understanding of the surrounding, they were not very popular until recently. Most of the interaction conscious networks used to be Dynamic Bayesian [9, 10] or prototype trajectory models [11]. However, several models have been introduced more recently, taking advantage of surrounding information for trajectory prediction. Many architectures use Long short-term memory (LSTM) neural networks [12, 13, 14] to capture the information of the neighboring vehicles. In the famous work by Deo *et al.* [4], the encoded information for each vehicle is condensed into a single tensor. Convolutional and max-pooling layers follow it to avoid generalization and failure to address complicated scenarios. This information is concatenated with LSTM encoding of the target vehicle and passed to a Maneuver-based LSTM decoder that forecasts multiple trajectories based on maneuver classes discussed in [4].

In [15], Mercat *et al.* also use LSTM based encoder-decoder architecture but avoid using predefined maneuver classes. It has self-attention layers in the middle that accept the encoded information of each vehicle for specific time instances. This helps in generating a fixed-sized input even when the number of vehicles in the scene might change. The middle layer produces an attention matrix based on the features extracted from the encoder. Finally, the decoder predicts path probabilities for each vehicle in the scene. The performance of LSTM based model in [15] is better than most of the best in class trajectory predicting algorithms. However, graph neural networks (GNN) with unique learning ability and have been able to produce higher accuracy results when applied to path prediction [7, 16].

The work by Xie. *et al.* [7] proposes a GNN [17] based teacher-student model that predicts higher accuracy trajectories than the previous models. The teacher model accepts frame-wise graph input built to reflect the positions of all the agents in the input frame. It also uses Graph Convolutional network-based encoder-decoder for generative learning and Gaussian mixture model for congestion pattern generation. The student model uses LSTM based encoder-decoder for trajectory prediction and matches the congestion pattern of the teacher model to improve the accuracy of prediction.

The improving error rates for deep learning algorithms predicting vehicle trajectory are routinely focused on in most published research. We have successfully attained error rates comparable to state-of-the-art algorithms with lower model complexity and smaller model size. We use ATCN based novel encoder to grasp the positions of the vehicles in the scene for the past three seconds as compared to LSTM encoders in modern models [7, 15]. The output of encoders is used to condense the details of vehicular interaction in the past using 2D convolution. This information is passed to the LSTM Trajectory predictor that predicts a vicinity-aware trajectory for the target vehicle for five seconds in the future. We used US Highway 101 [18], and Interstate 80 Freeway [19] datasets provided by the Federal Highway Administration (FHWA) under Next Generation Simulation (NGSIM) program for training and validating the model.

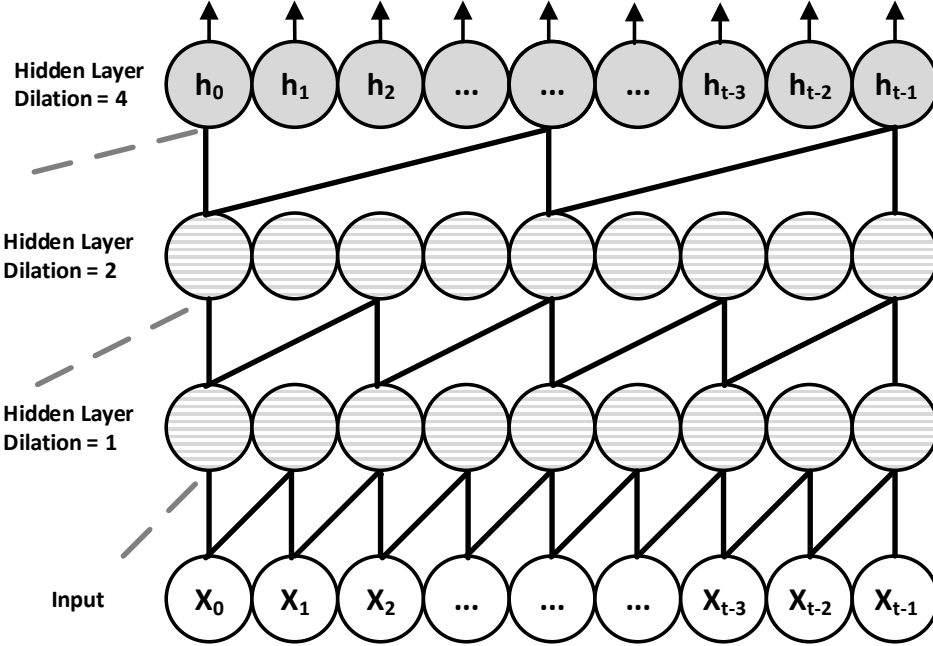


Figure 1: Dilated Causal Convolution.

3 DeepTrack

We first briefly explain ATCN in this section, and then we formulate the problem and explain the DeepTrack model.

3.1 Agile Temporal Convolutional Networks (ATCN)

Traditional Convolutional Neural Networks (CNN) are used in computer vision applications due to their success in capturing the spatial features within a two-dimensional frame. Recently, research has shown that specialized CNNs are capable of recognizing patterns in data history in order to predict future observations. This gives researchers interested in time-series forecasting options to choose from over RNNs, which have been regarded in the community as the established DNN for time-series predictions. In one such case, TCN have been shown to achieve state of the art accuracy in sequence tasks, i.e. polyphonic music modeling, word and character-level language modeling, and audio synthesis [20, 21, 22, 23, 24]. TCNs are designed around two basic principles: 1) the convolutional operations are causal, i.e., predictions are made based only on current and past information; 2) the network receives an input sequence of arbitrary length and maps it to an output sequence of the same length [24]. Currently, these simple causal convolutions have a dilation rate of 1, but other researchers incorporate dilated convolutions, shown in Fig. 1, to scale the receptive field exponentially. The dilated convolution of F on element s of a sequence X is given as:

$$F(s) = (x *_d f)(s) = \sum_{i=0}^{k-1} f(i) \cdot x_{s-d \cdot i}, \quad (1)$$

where $X \in \mathbb{R}^n$ is a 1-D input sequence, $*_d$ is dilated convolution operator, $f : \{0, \dots, k-1\} \in \mathbb{R}$ is a kernel of size k and d is the dilation rate [24]. Also receptive field of a dilated convolution can be calculated by:

$$rf = 1 + \sum_{j=1}^L [k(j) - 1] \times d(j), \quad (2)$$

where $j \in \{1, 2, 3, \dots, L\}$ is the layers, k is the kernel size, and $d(j)$ is the dilation rate at layer j . This means that as the depth of the network increase, so does the receptive field.

Inspired by TCN, we propose ATCN to reduce model complexity and memory footprint. Fig. 2 shows the structure of ATCN. The model shown in Fig. 2 has three hidden layers indicated by H. The hidden layers have a padding block

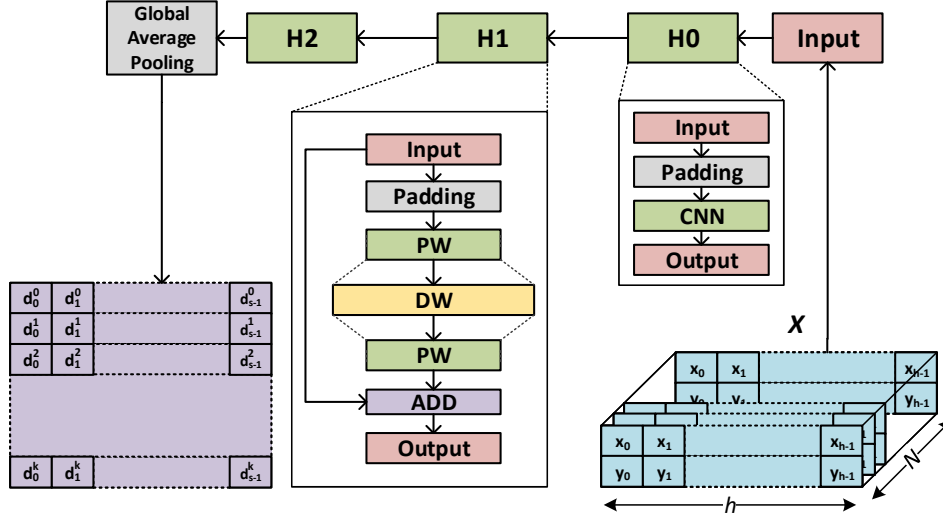


Figure 2: Structure of Agile Temporal Convolutional Networks (ATCN).

to extend input feature to ensure that the input and output of the convolution have the same length to satisfy principle number 2. In H0, we use the normal convolution operator, but in the subsequent layers (H1-H2), we remove the standard convolution and use pointwise (PW), depthwise (DW), and then another pointwise to reduce the model size and number of operations. In this research, we also added a Batch Normalization (BN) layer after each convolution to speed up and stabilize the model training. There is also a Swish as an activation function after each BN. To our best of the knowledge, this is the first time a vehicle trajectory model based on ATCN is presented. In the section 4, we show off the effect of ATCN network on the performance of DeepTrack both on accuracy and model complexity.

3.2 Problem formulation

The input of DeepTrack is define as:

$$\mathbf{X} = \begin{bmatrix} l_0^{t-h} & l_0^{t_1-h} & \dots & l_0^{t_0} \\ \vdots & \vdots & \ddots & \vdots \\ l_e^{t-h} & l_e^{t_1-h} & \dots & l_e^{t_0} \\ \vdots & \vdots & \ddots & \vdots \\ l_{N-1}^{t-h} & l_{N-1}^{t_1-h} & \dots & l_{N-1}^{t_0} \end{bmatrix}, \quad (3)$$

where $l_i^t = \langle x_i^t, y_i^t \rangle$ is the position of vehicle i at time t , and N is the number of vehicles. A car of interest is designated by the index e in \mathbf{X} . The shape of \mathbf{X} is shown in Fig. 2. To make fair comparisons, we construct \mathbf{X} for vehicle e similarly to what Deo *et al.* explained in [4]. In a similar way, the output can be defined as follows:

$$\hat{\mathbf{Y}} = [l^{t_1}, l^{t_2}, \dots, l^{t_f}]. \quad (4)$$

3.3 Model architecture

An illustration of the DeepTrack model can be found in Fig. 3. The model consists ATCN encoder, Vehicular Interactive Aware Convolution (VIAC), and LSTM trajectory encoder. In the next section, we explain the structure of each component.

3.3.1 ATCN encoder

ATCN encoders embed vehicles' path histories, both neighbors and ego vehicle, into higher dimensions in order to capture their past trajectory. As opposed to previous works [7, 4], ATCN does not require dense layers to embed input features as needed for the LSTM encoder. ATCN convolutional operators capture and map the sequence of l^t by

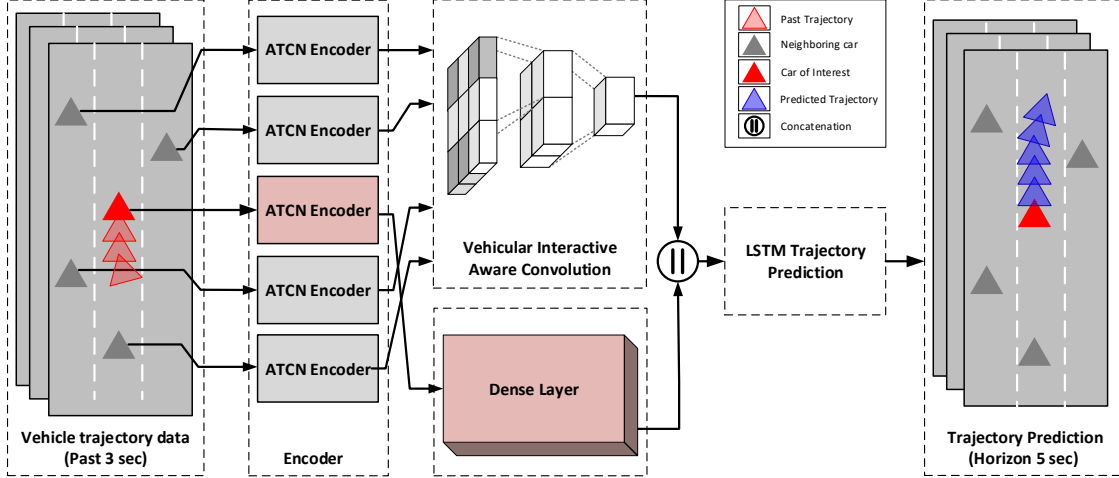


Figure 3: Overview of the trajectory prediction model. The location of the neighbors (gray triangles) and car of interest (solid red triangle) is shown at t_0 in Vehicle trajectory data (extreme left) block and Trajectory prediction (extreme right) block. Triangles denoting semi-transparent red in Vehicle trajectory data block, and semi-transparent blue in Trajectory prediction block represent observed history paths, and model output respectively. The observed history paths of neighbours (for past 3 seconds) are used by the model but not shown in the figure to avoid confusion.

applying $K = [2, k]$ as a kernel, where $k \in \mathbb{R} | k \leq h$. As a result, DeepTrack has less model complexity, and better gradients flow from output to input during optimization.

DeepTrack uses two different ATCN encoders. There is one ATCN shared by all neighbors, shown by the shaded box in Fig. 3, which maps their dynamics to higher dimensions so that the VIAC can comprehend their interdependencies. As illustrated by the red box in Fig. 3, the other ATCN maps only the ego dynamics.

Since we have a padding unit in each ATCN to make sure the input and output of standard and depthwise convolution will be same, the $2p$ zeros are added symmetrically, where p is given by:

$$p = \lceil \frac{(o - 1) \times s + (k - 1) \times (d - 1) - i + k}{2} \rceil, \quad (5)$$

where o is the output size, i is the input size, s is the stride, k is the kernel, and d is the dilation. According to Eq. 5, if we increase the kernel size or dilation, more zeros should be padded to the input. The addition of excessive zeros to the input has two main disadvantages: ① it degrades the model’s performance due to redundant zeros, and ② it increases the model computational complexity. As a result, we set the dilation rate and kernel size to 1, 2, respectively. In Table 1, both ATCN encoders have three hidden layers; however, the output dimensions differ.

Table 1: Configuration of ATCN encoder for ego and neighbors

ATCN Encoder	Configurations (H0, H1, H2)		
	Output feature dimensions	Dilation rate	Kernel size
Neighbours	[16, 32, 64]	[1, 1, 1]	[2, 2, 2]
Ego	[8, 16, 32]	[1, 1, 1]	[2, 2, 2]

3.3.2 VIAC

An analysis of the interaction between the ego and its surrounding neighbors is necessary to predict the future trajectory of the vehicle of interest. Despite being able to capture individual behavior, the ATCN encoder is unable to comprehend the entire scene. Social pooling [25] proposes a solution by pooling encoded data around a specific target. The task is accomplished by defining a spatially correlated grid $f \times g \times N$ in respect to the car of interest. Similar to the work of

[4], we set f and g to 13 and 3, respectively. Fig.3 shows the structure of the grid for the shape of 3x3, which masked the ATCN encoded output.

DeepTrack comprehends the interdependencies of the vehicle by applying convolutions to embeds information. The neighborhood dynamics are encoded and mapped to the lower dimension using the two-layer convolution and a pooling unit. The dense layer also remaps the ATCN encoder output of ego to have the same feature size so that it can be concatenated with the result of VIAC.

3.4 LSTM decoder

In the final stage, the LSTM decoder receives the concatenated ego dynamics and neighbors' interdependencies to predict the future trajectory of the car of interest, \hat{Y} . We have not used ATCN as the final stage because the ATCN is the only cable to map the temporal information to a higher output channel. Similar to what is accomplished by the ATCN encoder at the first stage. Due to the mapping of all features to higher output channel dimensions, LSTM still needs to map and decode the output of the VIAC and ego ATCN encoders to the final output prediction.

4 Evaluation

4.1 Datasets

The performance of our model has been evaluated using NGSIM I-80 and US-101, two well-known, widely available vehicle trajectory datasets. A sampling rate of 10 Hz is used for sampling the trajectory of the vehicle over a period of 45 minutes. Each dataset includes three segments of 15 minutes long of mild, moderate, and congested traffic.

Similarly to [4], we divided the dataset into three parts: training, validation, and testing. This chapter reports the results of analyzing the test sets. Based on the work of [4], each trajectory is also segmented into 8 seconds, where the first three seconds are used as a path that was observed, and the model will predict the following five seconds. To reduce the complexity of the LSTM encoder, previous works downsampled each second by two [4, 7, 15]. While we are not limited to this fact, we also downsampled the inputs to have a fair comparison. In Fig. 4(a)-5, the location of the neighbors (gray triangles) are shown at t_0 . Triangles denoting red, green, and blue respectively, represent observed history paths, ground truth, and model output.

4.2 Implementation Details

The model is implemented in PyTorch and trained on an Nvidia Tesla V100 GPU using the ADAM optimizer with a Learning Rate (LR) of 0.001 with a gradient clip of 10. Additionally, the LR is reduced by an additional factor of 0.1 if the validation loss remains stagnant for two epochs. The total number of epochs was set to 10.

4.3 Metric

To provide a fair comparison to other works, we used an error metric called Root Mean Square Error (RMSE) to assess the overall performance of the system. The RMSE at time t is given by:

$$RMSE^t = \sqrt{\frac{1}{N} \sum_{i=1}^N (Y_i^t - \hat{Y}_i^t)^2}, \quad (6)$$

where Y is the ground truth, \hat{Y} is predicted output, and N is number of samples. We also use the Average Displacement Error (ADE) to compare the average RMSE over 5 seconds.

4.4 Quantitative Results

A comparison of DeepTrack against off-the-shelf algorithms on the NGSIM dataset was conducted for the purpose of providing a comprehensive comparison. The results are listed in Table 2. Compared to CS-LSTM and its other variant CS-LSTM (M), DeepTrack can reduce ADE by 9.09% and 11.56%, respectively. It is due to the fact that our ATCN has higher gradient stability that it is better able to generalize solutions. However, both CF-LSTM and SAAMP outperformed the DeepTrack for 0.87% and 4.21%. SAAMP's attention mechanism allows it to gain a better understanding of certain interactions, thereby improving the overall RMSE.

Considering that the final model will be deployed on the vehicle, model complexity is another important metric that previous researchers have overlooked. Therefore, we analyzed and compared the model complexity as measured by

the number of Multiply-Accumulate (MAC) operations and the size of the model parameters for three approaches in Table 3. Since the source code for SAAMP was not available publicly, we could not compare its model complexity with DeepTrack. The smaller model size means a lower memory footprint on the final hardware. Low MACs also translates into better execution performance on the same hardware. As we can see, DeepTrack is able to improve the MACs and size of the model by 11.47% and 19.22%, respectively, over CF-LSTM. In addition to improving ADE over CS-LSTM, DeepTrack also improved MACs by 10.49% and model size by 18.5%.

Table 2: Performance comparison based on NGSIM dataset. RMSE is calculated in meters.

Model	RMSE (m)					ADE
	1 sec	2 sec	3 sec	4 sec	5 sec	
CS-LSTM [4]	0.61	1.27	2.09	3.1	4.37	2.29
CS-LSTM (M) [4]	0.62	1.29	2.13	3.2	4.52	2.35
CF-LSTM [7]	0.51	1.13	1.88	2.81	3.98	2.06
SAAMP [15]	0.55	1.1	1.78	2.73	3.82	2.00
DeepTrack	0.43	1.12	1.91	2.87	4.07	2.08

Table 3: Model size and number of flops per model

Parameters	Models		
	CF-LSTM [7]	CS-LSTM [4]	DeepTrack
MACs	2,064,282	2,045,938	1,667,425
Parameters	193,941	191,829	171,703

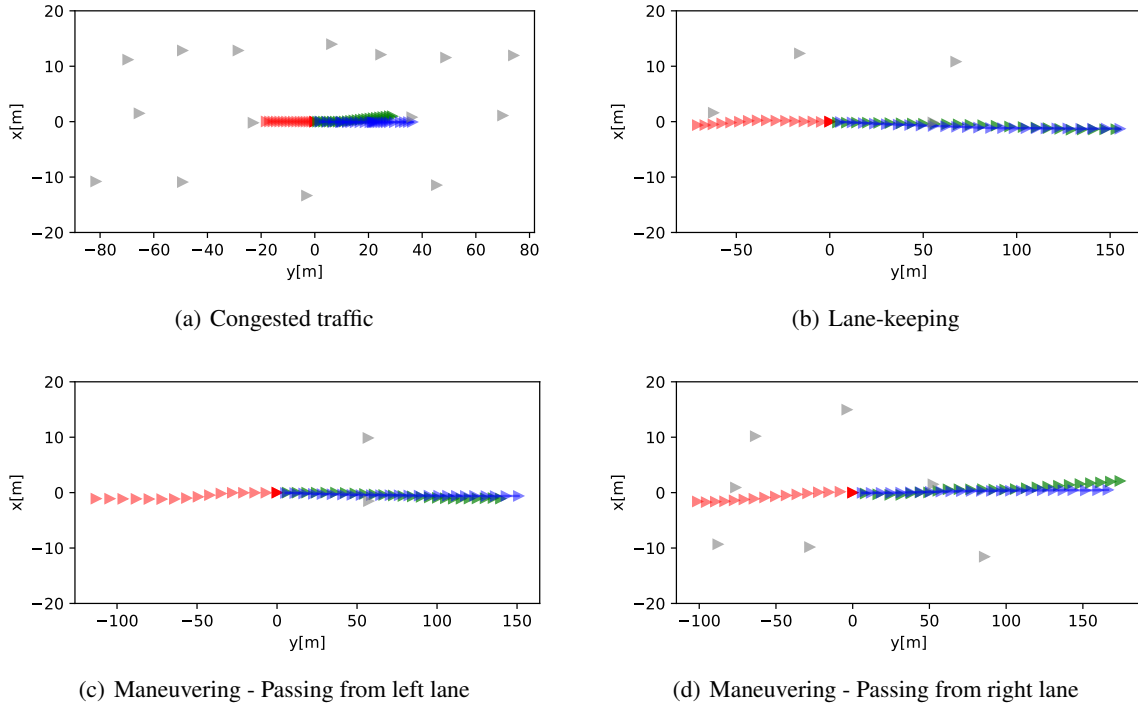


Figure 4: The location of the neighbors (gray triangles) is shown at t_0 . Triangles denoting red, green, and blue respectively, represent observed history paths, ground truth, and model output.

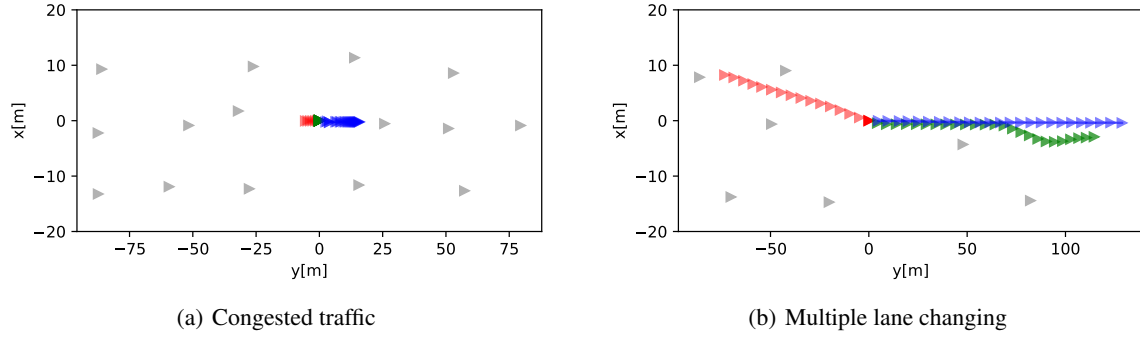


Figure 5: Two cases where the model failed to predict the trajectory precisely due to unpredictable driver behaviour. Same legend is used as Fig. 4.

4.5 Qualitative Results

The model predicted output for four scenarios is shown as an aid to understanding the model behaviour: ① congested traffic (Fig. 4(a)), ② lane-keeping (Fig. 4(b)), ③ maneuvering and passing a car from left lane (Fig. 4(c)), ④ maneuvering and passing a car from right lane (Fig. 4(d)), and ⑤ cases where the model failed to predict the trajectory precisely (Fig. 5). The three types of the path shown in red, green, and blue triangles represent path history, ground truth, and predicted trajectory for the designated vehicle. The location of the neighbors (gray triangles) is also shown at t_0 . For the sake of simplicity, we didn't show the neighbors history path.

The comparison of Fig. 4(a) and Fig. 4(b) shows that the model can accurately estimate the velocity of the interest car based on the ego history. The model correctly predicted that vehicles would travel less distance as a result of congested traffic. The vehicle in the lane-keeping scenario travels farther, and DeepTrack has interfered with the same behavior. Figures 4(c) and 4(c) illustrate how DeepTrack performs when a car of interest passes its front vehicle from either the left or the right lane. Fig. 5 shows the scenarios in which DeepTrack was not able to predict the trajectories due to uncertainty in driver behavior. In the congested scenario (Fig. 5(a)), although the driver slowly drove his car until t_0 , the vehicle stopped for the entire next five seconds, while the model predicts it would come close to the front car. An alternative scenario (Fig. 5(b)) involves the vehicle being steered into the right lane. The model predicted that the vehicle would keep the lane and accelerate for the next five seconds; however, the driver has decided to change the lane another time. In this case, the model did not capture this behaviour since the maneuver occurred during the prediction horizon.

5 Conclusion and Future Works

DeepTrack is an agile deep learning model with comparable accuracy to best-in-class trajectory prediction algorithms but with much smaller model size and lower computational complexity suitable for embedded edge systems. The vehicle dynamics are encoded using ATCN instead of LSTM units in DeepTrack. ATCN utilizes depthwise convolution, thereby reducing the complexity of models both in terms of size and operations when compared with LSTMs. Our experimental results indicate that DeepTrack reduces prediction error by 9.09% and 11.56%, respectively, and reduces the number of operations and model size by about 10.49% and 18.5%, respectively, to CS-LSTM. With similar ADE to CF-LSTM, DeepTrack can also reduce the number of operations and model size by 10.49% and model size by 18.5%.

We plan to work on two aspects as future works: First, we believe tagging geological meta information will improve the performance of DeepTrack on multiple lanes changing. If the vehicle is near an exit, it is more likely to change lanes repeatedly. Secondly, both CF-LSTM and CS-LSTM downsampled the input history to reduce the LSTM complexity and have better training performance. Due to DeepTrack's replacement of LSTM with ATCN, we have no bounds anymore, so we can take advantage of a larger sample size to improve DeepTrack's performance.

References

- [1] (2019) Fatality Analysis Reporting System (FARS), Motor vehicle traffic crashes (1994-2019). [Online]. Available: <https://www-fars.nhtsa.dot.gov/Main/index.aspx>

- [2] (2019) Fatality Analysis Reporting System (FARS), Vehicles involved in fatal crashes. [Online]. Available: VehiclesInvolvedinFatalCrashes, <https://www-fars.nhtsa.dot.gov/Vehicles/VehiclesAllVehicles.aspx>
- [3] V. D. H. Richard and H. Jeroen, “Time-to-Collision and Collision avoidance systems,” *International Cooperation on Theories and Concepts in Traffic safety (ICTCT)*, 1994.
- [4] N. Deo and M. M. Trivedi, “Convolutional social pooling for vehicle trajectory prediction,” in *2018 IEEE Conference on Computer Vision and Pattern Recognition Workshops, CVPR Workshops 2018, Salt Lake City, UT, USA, June 18-22, 2018*. IEEE Computer Society, 2018, pp. 1468–1476.
- [5] T. Phan-Minh, E. C. Grigore, F. A. Boulton, O. Beijbom, and E. M. Wolff, “Covernet: Multimodal behavior prediction using trajectory sets,” in *2020 IEEE/CVF Conference on Computer Vision and Pattern Recognition, CVPR 2020, Seattle, WA, USA, June 13-19, 2020*. IEEE, 2020, pp. 14 062–14 071. [Online]. Available: <https://doi.org/10.1109/CVPR42600.2020.01408>
- [6] L. Hou, L. Xin, S. E. Li, B. Cheng, and W. Wang, “Interactive trajectory prediction of surrounding road users for autonomous driving using structural-lstm network,” *IEEE Trans. Intell. Transp. Syst.*, vol. 21, no. 11, pp. 4615–4625, 2020. [Online]. Available: <https://doi.org/10.1109/TITS.2019.2942089>
- [7] X. Xie, C. Zhang, Y. Zhu, Y. N. Wu, and S. Zhu, “Congestion-aware multi-agent trajectory prediction for collision avoidance,” *CoRR*, vol. abs/2103.14231, 2021. [Online]. Available: <https://arxiv.org/abs/2103.14231>
- [8] S. Lefèvre, D. Vasquez, and C. Laugier, “A survey on motion prediction and risk assessment for intelligent vehicles,” *ROBOMECH journal*, vol. 1, no. 1, pp. 1–14, 2014.
- [9] E. Kafer, C. Hermes, C. Wöhler, H. J. Ritter, and F. Kummert, “Recognition of situation classes at road intersections,” in *IEEE International Conference on Robotics and Automation, ICRA 2010, Anchorage, Alaska, USA, 3-7 May 2010*. IEEE, 2010, pp. 3960–3965. [Online]. Available: <https://doi.org/10.1109/ROBOT.2010.5509919>
- [10] A. Lawitzky, D. Althoff, C. F. Passenberg, G. Tanzmeister, D. Wollherr, and M. Buss, “Interactive scene prediction for automotive applications,” in *2013 IEEE Intelligent Vehicles Symposium (IV), Gold Coast City, Australia, June 23-26, 2013*. IEEE, 2013, pp. 1028–1033. [Online]. Available: <https://doi.org/10.1109/IVS.2013.6629601>
- [11] M. Brand, N. Oliver, and A. Pentland, “Coupled hidden markov models for complex action recognition,” in *1997 Conference on Computer Vision and Pattern Recognition (CVPR '97), June 17-19, 1997, San Juan, Puerto Rico*. IEEE Computer Society, 1997, pp. 994–999. [Online]. Available: <https://doi.org/10.1109/CVPR.1997.609450>
- [12] W. Kun, W. Shaobo, Z. Pan, Y. Biao, H. Weixin, and L. Huawei, “Vehicle trajectory prediction by knowledge-driven lstm network in urban environments,” 2020. [Online]. Available: <https://doi.org/10.1155/2020/8894060>
- [13] L. Lin, W. Li, H. Bi, and L. Qin, “Vehicle trajectory prediction using lstms with spatial-temporal attention mechanisms,” *IEEE Intelligent Transportation Systems Magazine*, pp. 0–0, 2021.
- [14] L. Xin, P. Wang, C. Chan, J. Chen, S. E. Li, and B. Cheng, “Intention-aware long horizon trajectory prediction of surrounding vehicles using dual LSTM networks,” in *21st International Conference on Intelligent Transportation Systems, ITSC 2018, Maui, HI, USA, November 4-7, 2018*, W. Zhang, A. M. Bayen, J. J. S. Medina, and M. J. Barth, Eds. IEEE, 2018, pp. 1441–1446. [Online]. Available: <https://doi.org/10.1109/ITSC.2018.8569595>
- [15] J. Mercat, T. Gilles, N. E. Zoghby, G. Sandou, D. Beauvois, and G. P. Gil, “Multi-head attention for multi-modal joint vehicle motion forecasting,” in *2020 IEEE International Conference on Robotics and Automation, ICRA 2020, Paris, France, May 31 - August 31, 2020*. IEEE, 2020, pp. 9638–9644. [Online]. Available: <https://doi.org/10.1109/ICRA40945.2020.9197340>
- [16] M. Mendieta and H. Tabkhi, “CARPe posterum: A convolutional approach for real-time pedestrian path prediction,” in *Thirty-Fifth AAAI Conference on Artificial Intelligence, AAAI 2021, Thirty-Third Conference on Innovative Applications of Artificial Intelligence, IAAI 2021, The Eleventh Symposium on Educational Advances in Artificial Intelligence, EAAI 2021, Virtual Event, February 2-9, 2021*. AAAI Press, 2021, pp. 2346–2354. [Online]. Available: <https://ojs.aaai.org/index.php/AAAI/article/view/16335>
- [17] K. Xu, W. Hu, J. Leskovec, and S. Jegelka, “How powerful are graph neural networks?” in *7th International Conference on Learning Representations, ICLR 2019, New Orleans, LA, USA, May 6-9, 2019*. OpenReview.net, 2019. [Online]. Available: <https://openreview.net/forum?id=ryGs6iA5Km>
- [18] J. Colyar and J. Halkias. (2007) Next generation simulation (NGSIM), US Highway-101 dataset. FHWA-HRT-07-030. [Online]. Available: <https://www.fhwa.dot.gov/publications/research/operations/07030/>
- [19] ——. (2006) Next generation simulation (NGSIM), Interstate 80 freeway dataset. FHWA-HRT-06-137. [Online]. Available: <https://www.fhwa.dot.gov/publications/research/operations/06137/>

- [20] A. van den Oord, S. Dieleman, H. Zen, K. Simonyan, O. Vinyals, A. Graves, N. Kalchbrenner, A. W. Senior, and K. Kavukcuoglu, “Wavenet: A generative model for raw audio,” *CoRR*, vol. abs/1609.03499, 2016. [Online]. Available: <http://arxiv.org/abs/1609.03499>
- [21] N. Kalchbrenner, L. Espeholt, K. Simonyan, A. van den Oord, A. Graves, and K. Kavukcuoglu, “Neural machine translation in linear time,” *CoRR*, vol. abs/1610.10099, 2016. [Online]. Available: <http://arxiv.org/abs/1610.10099>
- [22] J. Gehring, M. Auli, D. Grangier, and Y. N. Dauphin, “A convolutional encoder model for neural machine translation,” *CoRR*, vol. abs/1611.02344, 2016. [Online]. Available: <http://arxiv.org/abs/1611.02344>
- [23] J. Gehring, M. Auli, D. Grangier, D. Yarats, and Y. N. Dauphin, “Convolutional sequence to sequence learning,” *CoRR*, vol. abs/1705.03122, 2017. [Online]. Available: <http://arxiv.org/abs/1705.03122>
- [24] S. Bai, J. Z. Kolter, and V. Koltun, “An empirical evaluation of generic convolutional and recurrent networks for sequence modeling,” *CoRR*, vol. abs/1803.01271, 2018. [Online]. Available: <http://arxiv.org/abs/1803.01271>
- [25] A. Alahi, K. Goel, V. Ramanathan, A. Robicquet, L. Fei-Fei, and S. Savarese, “Social lstm: Human trajectory prediction in crowded spaces,” in *Proceedings of the IEEE conference on computer vision and pattern recognition*, 2016, pp. 961–971.